Available online at www.sciencedirect.com
ScienceDirect
Ceramics International 34 (2008) 1261–1265
CERAMICS INTERNATIONAL
www.elsevier.com/locate/ceramint

Effect of Ru and $LaNiO_3$ barrier layers on lead zirconate titanate films grown on nickel-based metal foils by sol–gel process

Dong-Joo Kim [a,*], Dongna Shen [a], Sang H. Yoon [a], Song-Yul Choe [b], David Y. Kaufman [c]

[a] *Materials Research and Education Center, Department of Mechanical Engineering, Auburn University, Auburn, AL 36849, USA*
[b] *Department of Mechanical Engineering, Auburn University, Auburn, AL 36849, USA*
[c] *Energy Technology Division, Argonne National Laboratory, Argonne, IL 60439, USA*

Received 26 January 2007; received in revised form 24 February 2007; accepted 4 March 2007

Abstract

Lead zirconate titanate [$Pb(Zr_{0.52}, Ti_{0.48})O_3$ (PZT)] films were grown by sol–gel process on nickel and hastelloy foils. PZT perovskite phase was obtained at 650 °C annealing condition and surface topography showed uniform and dense microstructure. The characterization on dielectric properties indicates that diffusion of foil elements into the PZT and the formation of low capacitance interfacial layer occur during process. In order to reduce the diffusion effect of foil element and/or interfacial layer, barrier layers such as $Ru(RuO_2)$ and $LaNiO_3$ layers were utilized on foil substrates. The increase of grain size was observed in PZT films grown on barrier layers. Dielectric properties are greatly improved without degrading ultimate dielectric breakdown strength.

Keywords: A. Sol–gel processes; C. Dielectric properties; D. PZT; Barrier layer

1. Introduction

Lead zirconate titanate (PZT) is ferroelectric oxide ceramic whose excellent dielectric, piezoelectric, and ferroelectric properties make it very interesting for a large number of applications [1]. Integration of PZT films on base metals can provide an important extension of ferroelectric ceramic oxide into various devices such as capacitive components, sensors and actuators [2,3]. With respect to capacitor application, factors desired for improving capacitor technology include higher capacitance density, higher dielectric breakdown strength, decreased electrical and thermal losses, improved reliability, and lower-cost electrode materials. One attractive approach to achieve these enhancements is to utilize thin film ferroelectric materials as the dielectric. Thin film dielectric layers can exhibit improved materials uniformity, higher density, and smoother electrode–dielectric interfaces, all of which can lead to higher breakdown strength. Additionally, the extremely fine microstructure typical of thin films, coupled with mechanical clamping of the dielectric thin film by the substrate, can result in improved temperature stability. Thin film technologies can also reduce device footprints and permit integration directly onto micro-circuitry. The integration with base metal substrates provides cost effective engineering process by replacing high cost of oxidation resistant electrodes such as Pt, Ag–Pd, and Au. However, development of thin film integration on metallic substrates has been complicated by oxidation of the base metal electrode [4–7].

In this paper, we report the $Pb(Zr_{0.52}, Ti_{0.48})O_3$ (PZT) films on nickel and nickel-based alloy, i.e. hastelloy foils prepared by sol–gel process. Electrical and structural properties of PZT films on foil substrates were examined with an emphasis on the effect of barrier layers.

2. Experimental

$Pb(Zr_{0.52}, Ti_{0.48})O_3$ (PZT) films were prepared by sol–gel process. Sol–gel process was chosen due to its technical advantages such as cost effective coating, ease of chemical composition control, and large area coverage. Lead acetate trihydrate [$Pb(O_2C_2H_3)_2 \cdot 3H_2O$], titanium isopropoxide [($Ti(OC_3H_7)_4$], and zirconium *n*-propoxide [$Zr(OC_3H_7)_4$] were

---

* Corresponding author.
E-mail address: dkim@eng.auburn.edu (D.-J. Kim).

doi:10.1016/j.ceramint.2007.03.017

used as starting precursors. 2-Methoxyethanol was used as a solvent for all precursors. Mole concentration of solution for coating was 0.5 mol, and Zr to Ti ratio was set to 0.52–0.48. PZT layers were prepared by spin-coating the stock solution onto metallic foils at 2500 rpm for 30 s. Each PZT layer was pyrolyzed at 450 °C for 10 min. After two layers were deposited (∼225 nm) and pyrolyzed, the film was annealed at 650 °C for 8 min through direct insertion into a tube furnace. Final annealing after obtaining the desired film thickness was performed at 650 °C for 20 min in air to ensure full transformation into the perovskite phase. Nickel and hastelloy C-276 were used as substrates after polishing surfaces of 500 μm foils. Either of two barrier layers, $LaNiO_3$ or Ru, was deposited on bare foil surface prior to deposition of the PZT film. $LaNiO_3$ layers were deposited by sol–gel process. Lanthanum nitrate and nickel acetate were dissolved in 2-methoxyethanol. The deposited $LaNiO_3$ films were annealed at 600 °C for 30 min, and were nominally 150 nm. Ru layers were coated by sputter deposition at room temperature with a thickness of about 100 nm.

For electrical characterization, 100 nm thick platinum top electrodes were deposited by e-beam evaporation to define 750 μm diameter capacitors. Dielectric properties such as dielectric constant and loss tangent (tan δ) were measured using an HP 4192A impedance analyzer with an oscillation signal of $0.1 V_{RMS}$ at 10 kHz. The dielectric breakdown strength and leakage current were measured using a Keithley 237 source-measurement unit. The surface morphology of the films was characterized by scanning probe microscope (SPM, JEOL JSM-700F). Phase identification was assessed by X-ray diffraction (XRD) utilizing Cu Kα radiation. The thermal properties of the gel powders were analyzed using differential scanning calorimeter/thermo-gravimetric analysis (DSC/TGA, Rheometric Scientific STA1500), with heating rate of 10 °C/min.

3. Results and discussion

Fig. 1 presents the DSC and TGA spectra of the dried $Pb(Zr_{0.52}, Ti_{0.48})O_3$ (PZT) gel powders. The initial 3% weight loss which occurs from room temperature to 160 °C is attributed to the evaporation of solvents such as water and alcohol. This is also accompanied by a broad and weak endothermic DSC peak. The following weight loss from 160 to 420 °C is mainly due to the removal and decomposition of organic groups. The peak around 270 °C in DSC curve is responsible for such reaction. The peak around 390 °C can correspond to the combustion reaction of organic compounds remaining up to this temperature. Broad exothermic DSC peak above 430 °C can correspond to the crystallization of amorphous PZT. For the entire thermal process, the percentage of mass reduction ranged up to 28%.

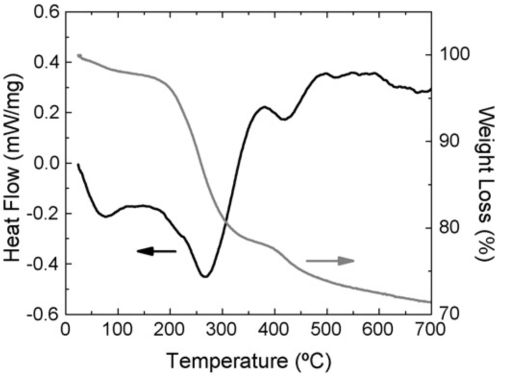

Fig. 1. DSC/TGA spectra of PZT gel powders.

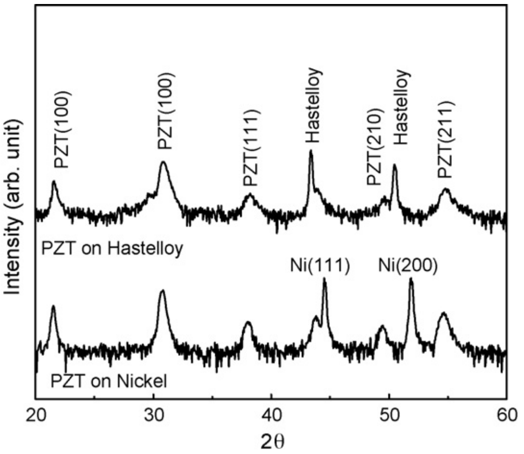

Fig. 2. X-ray diffraction patterns of PZT films deposited on nickel and hastelloy foil substrates.

Fig. 2 shows XRD plots of 0.9 μm thick PZT films deposited on nickel and hastelloy foil substrates. All diffraction peaks from the films were indexed as perovskite phase and substrate. Pyrochlore phase could not be identified in XRD data, and peaks corresponding to other metal oxide phase were not noticeable within the detection limit although interfacial oxide layers are expected to form in these films [4,8]. PZT films exhibit the polycrystalline with the strongest intensity of the (1 1 0) reflection and no significant difference was observed between nickel and hastelloy substrates. Fig. 3 shows the surface morphologies of the crystallized PZT films on nickel and hastelloy substrates. These surface topography show typical lateral surface grain size of around 70 nm and relatively conformal coverage under optimized sol–gel process.

Fig. 4(a) illustrates room temperature dielectric constants and loss tangents of 0.9 μm thick PZT films as a function of dc bias at 10 kHz. Values of the dielectric constant and loss tangent of PZT(52/48) on nickel and hastelloy were similar compared with those of PZT films deposited on metallic substrate [5,6]. However, when compared with those of PZT films deposited on platinized silicon substrates, dielectric constant exhibited lower values. This is attributed to the formation of an interfacial layer and diffusion of Ni, Cr, or Fe into PZT films. It is reported that the secondary phase such as $Pb_2(CrO_4)O$ was formed at the interface between PZT film and hastelloy substrate during annealing [8]. The effect of these deleterious processes on the total capacitor dielectric response can be evaluated by considering the series capacitor model. When the thickness variation in the dielectric constant is fitted to such a model, the measured capacitance of the film is expected by

$$\frac{1}{C_{meas}} = \frac{1}{C_{bulk}} + \frac{1}{C_{interface}} \quad (1)$$

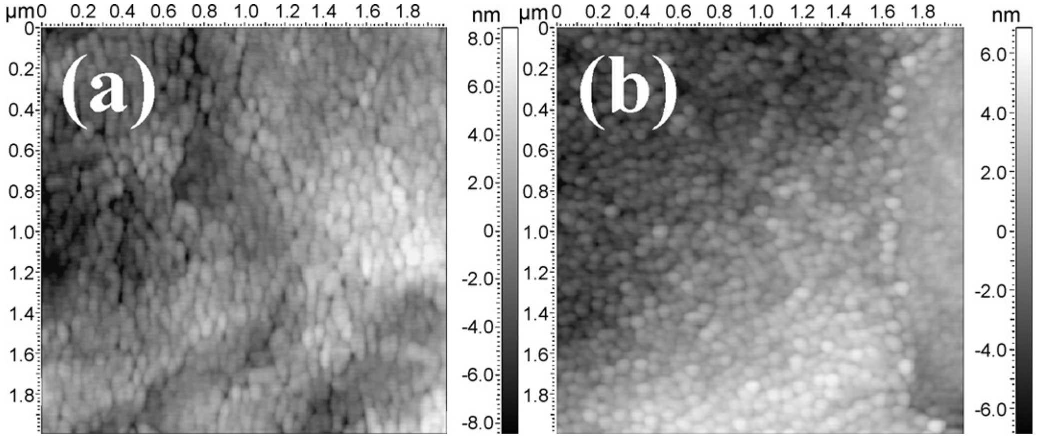

Fig. 3. Surface topography of PZT films on (a) nickel and (b) hastelloy. Film thickness is 0.9 μm, and pyrolyzed at 450 °C and annealed at 650 °C.

where C_{meas}, C_{bulk}, and $C_{\text{interface}}$ are referred to the measured, bulk, and interface capacitance, respectively. If the interfacial layer thickness $d_{\text{interface}}$ is independent of the total thickness d, then the equation is given by

$$\frac{d}{\varepsilon_{\text{meas}}}=\frac{d_{\text{bulk}}}{\varepsilon_{\text{bulk}}}+\frac{d_{\text{interface}}}{\varepsilon_{\text{interface}}}=\frac{d}{\varepsilon_{\text{bulk}}}+d_{\text{interface}}\left[\frac{1}{\varepsilon_{\text{interface}}}-\frac{1}{\varepsilon_{\text{bulk}}}\right]\approx\frac{d}{\varepsilon_{\text{bulk}}}+\frac{d_{\text{interface}}}{\varepsilon_{\text{interface}}} \qquad (2)$$

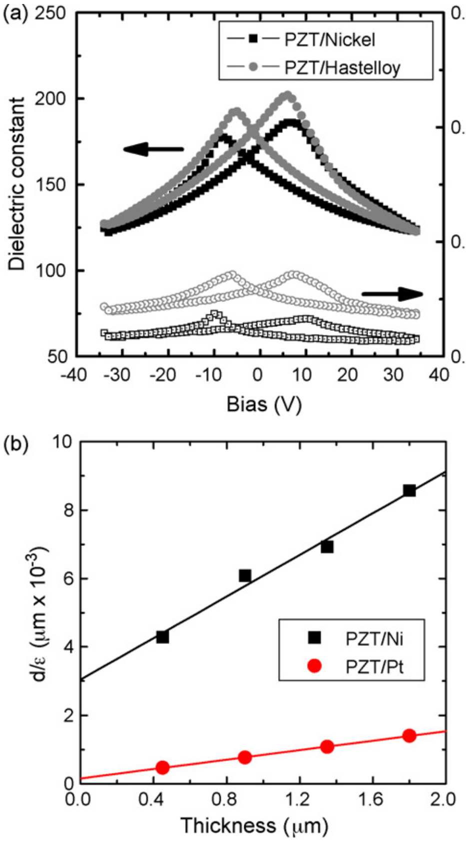

Fig. 4. (a) The dielectric constants and loss tangents of PZT films deposited foil substrates and (b) d/ε plots of PZT films on nickel foils and platinized silicon substrates. Film thickness is 0.9 μm, and pyrolyzed at 450 °C and annealed at 650 °C.

It is usually assumed that either $\varepsilon_{\text{bulk}} \gg \varepsilon_{\text{interface}}$ or $d_{\text{bulk}} \gg d_{\text{interface}}$, giving a linear relationship between $d/\varepsilon_{\text{meas}}$ and d with a slope of $1/\varepsilon_{\text{bulk}}$ and y-axis intercept of $d_{\text{interface}}/\varepsilon_{\text{interface}}$. Fig. 4(b) compares the inverse dielectric constant of PZT films deposited on nickel foils and on platinized silicon substrates. The y-axis intercept values of PZT films on nickel and platinum substrate were 3×10^{-3} and 0.12×10^{-3} μm, respectively. The bulk dielectric constants of PZT on nickel and platinum substrate, calculated from this plot, were 330 and 1520, respectively. This result indicates the extent of foil element diffusion into PZT, which lowered bulk permittivity. Another feature observed for PZT/Ni (alloy) foils was a more hysteretic response in the dielectric constant–voltage curves. For example, 0.9 μm PZT on Pt/SiO_2/Si shows a switching voltage around 2 V. However, PZTs on nickel or hastelloy show a switching voltage of around 6.5 V as shown in Fig. 4(a). This may also be attributed to the incorporation of foil element into PZT due to the diffusion during annealing. It is known that Ni, Cr, Fe elements can act as a hard doping of the PZT and increase the coercive voltage [9]. Low-K interfacial layer is also considered as reason for varying apparent switching voltage.

In order to prevent the diffusion between ferroelectric materials and metal foil substrates, barrier layers such and Ru and $LaNiO_3$ were used. Fig. 5 shows XRD patterns of 0.9 μm thick PZT films on nickel and hastelloy heterostructure foil substrates. Peaks from the PZT pervoskite phase, barrier layer of either LNO or RuO_2, and the substrate are present. PZT films deposited on the Ru-coated foil shows RuO_2 peak, indicating transformation of Ru into RuO_2 during thermal annealing of the PZT films. Orientation of PZT films on Ru(RuO_2) barrier layers show (1 1 0) orientation similar to plain nickel or hastelloy substrates, while PZT(52/48) films on $LaNiO_3$-coated foil show (1 0 0) orientation. Such orientation is due to the formation of PZT phase is favored by nucleation and growth on underlying (1 0 0)-oriented $LaNiO_3$ layers. The effect of barrier layers on microstructure of PZT films was characterized as shown in Fig. 6. The increase of grain size was observed for PZTs with Ru and $LaNiO_3$ compared with those on foils without barrier layers. Typical grain size of 0.9 μm thick PZT films was around 120–150 nm.

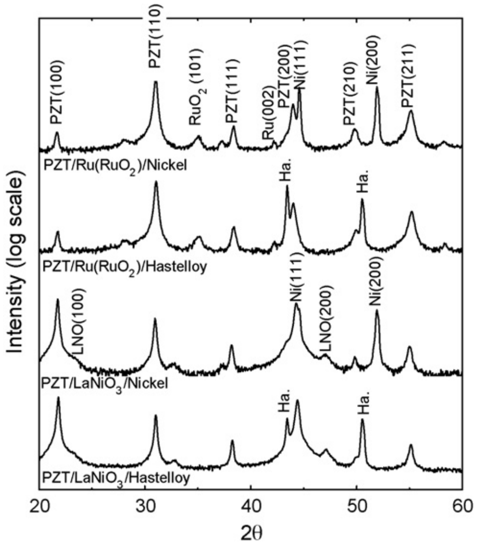

Fig. 5. X-ray diffraction patterns of PZT films with barrier layers (film thickness is 0.9 μm, pyrolyzed at 450 °C and annealed at 650 °C, Ha. = Hastelloy).

Room temperature dielectric constants and loss tangents were measured as a function of dc bias as shown in Fig. 7. Compared with values in Fig. 4(a), the dielectric properties are greatly improved in the films with barrier layers. The zero field dielectric constants of PZTs with the Ru barrier on nickel and hastelloy foils were 945 and 1015, respectively. Loss tangents for those films were around 6.5–7.6%. In case of $LaNiO_3$ barrier, the dielectric constants were 785 for nickel and 870 for hastelloy, and loss tangents were 4% and 5.3% for nickel and hastelloy foils, respectively. It is found that the utilization of barrier is very effective to improve dielectric properties by preventing diffusion of foil elements.

The ultimate dielectric breakdown strength under electrical bias were characterized for 0.9 μm thick PZT(52/48) films deposited on plain nickel foils with and without barrier layers as shown in Fig. 8. The breakdown voltages were 145 V (1.61 MV/cm) for PZT/nickel, 140 V (1.56 MV/cm) for PZT with $Ru(RuO_2)$/nickel, and 113 V (1.25 MV/cm) $LaNiO_3$/nickel. All values were much higher compared with bulk PZT ceramics (1 MV/cm) which is estimated from an empirical equation reported by Gerson and Marshall [10]. Such higher ultimate breakdown strength can be due to the uniform microstructure and high density of films produced by homogeneous chemical solution deposition. Slightly larger values observed in PZTs without barriers may be due to diffusion of foil elements such as Ni and/or Cr, which probably affects the donor doping effect on PZT films. In addition, voltage drop through interfacial layer may lead

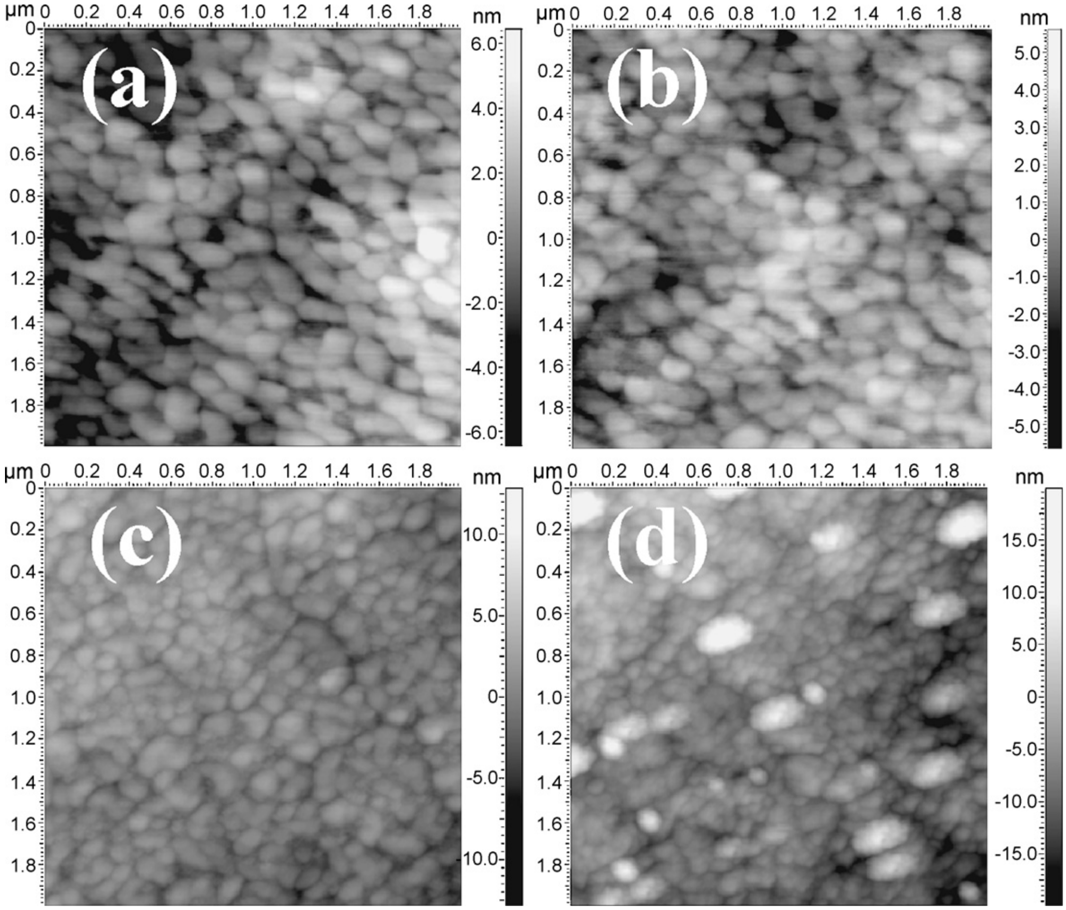

Fig. 6. Surface topography of 0.9 μm thick PZT films with $Ru(RuO_2)$ on (a) nickel and (b) hastelloy and with $LaNiO_3$ on (c) nickel and (d) hastelloy.

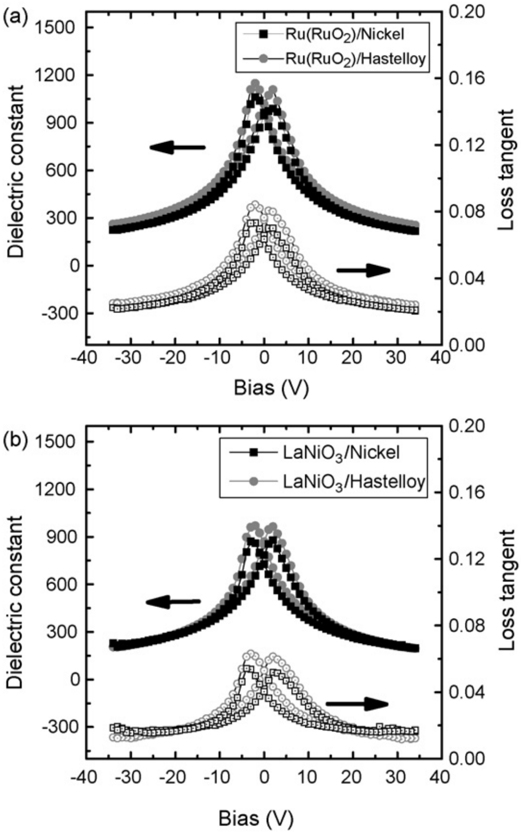

Fig. 7. The dielectric constants and loss tangents of PZT films with barrier layers as a function of dc bias: (a) Ru(RuO_2) and (b) $LaNiO_3$.

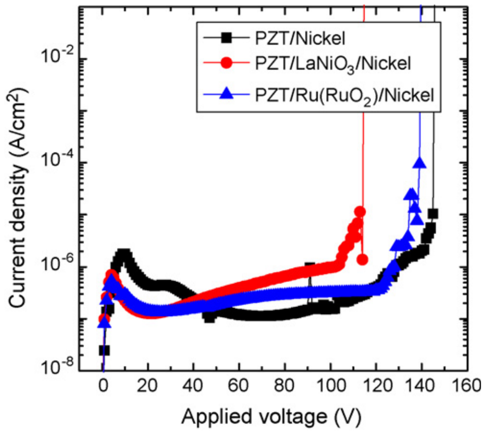

Fig. 8. Leakage current dependence on applied voltage of PZT films deposited on nickel foils with and without barrier layers.

to less voltage into the ferroelectric PZT layers, which results in higher breakdown voltage for the PZT without barrier layers. The incorporation of conductive oxide as barrier layers such as RuO_2 and $LaNiO_3$ was found to improve the dielectric properties without degrading breakdown field.

4. Conclusions

Ferroelectric $Pb(Zr_{0.52}, Ti_{0.48})O_3$ (PZT) films were grown by sol–gel process on nickel and hastelloy foil substrates. Under optimal annealing conditions to form perovskite phase from PZT sol–gel, surface topography showed uniform and dense microstructure with average grain size of around 70 nm at the film thickness of 0.9 μm. The dielectric constants of PZT films on foil substrates exhibited the values ranging from 170 to 180, and the loss tangents showed around 2.6–5%. It is considered that the diffusion of foil elements into the PZT and formation of low capacitance interfacial layer can be responsible. Dielectric properties were significantly improved by utilizing barrier layers such as RuO_2 transformed from Ru during annealing and conductive oxide electrode $LaNiO_3$. The increase of grain size was observed in PZT films with barrier layers. Ultimate breakdown strength of sol–gel processed PZT films was higher than that of bulk counter part. Therefore, sol–gel PZTs employing barrier layers is one potential process for achieving high performance ferroelectric films on base metal foil substrates for high performance capacitor fabrication.

Acknowledgements

This work was supported by Auburn University Detection and Food Safety Center, an Industry, the U.S. Department of Energy, FreedomCAR and Vehicle Technologies Program, and the National Science Foundation (through grant no. DMR-0605270).

References

[1] N. Setter, R. Waser, Electroceramic materials, Acta Mater. 48 (2000) 151–178.
[2] A.I. Kingon, S. Srinivasan, Lead zirconate titanate thin films directly on copper electrodes for ferroelectric, dielectric and piezoelectric applications, Nat. Mater. 4 (2005) 223–237.
[3] P.G. Mercado, A.P. Jardine, Smart thin film TiNi/piezoelectric heterostructure, J. Vac. Sci. Technol. A 13 (1995) 1017–1021.
[4] J.-P. Maria, K. Cheek, S.K. Streiffer, S.-H. Kim, G. Dunn, A.I. Kingon, Lead zirconate titanate thin films on base-metal foils: an approach for embedded high-permittivity passive components, J. Am. Ceram. Soc. 84 (2001) 2436–2438.
[5] K. Saegusa, Preparation and electrical properties of sol–gel derived lead zirconate titanate glass-ceramic thin films on metal foil substrate, Jpn. J. Appl. Phys. 36 (1997) 6888–6893.
[6] Q. Zou, H.E. Ruda, B.G. Yacobi, K. Saegusa, M. Farrell, Dielectric properties of lead zirconate titanate thin films deposited on metal foils, Appl. Phys. Lett. 77 (2000) 1038–1040.
[7] J.T. Dawley, P.G. Clem, Dielectric properties of random and ⟨1 0 0⟩ oriented $SrTiO_3$ and (Ba, Sr)TiO_3 thin films fabricated on ⟨1 0 0⟩ nickel tapes, Appl. Phys. Lett. 81 (2002) 3028–3030.
[8] A. Dutschke, J. Meinhardt, Characterization of the interface of PZT sol–gel layers on metallic substrates, Surf. Interf. Anal. 36 (2004) 1185–1189.
[9] Y. Xu, Ferroelectric Materials and Their Applications, Elsevier Science Pub. Co., The Netherlands, 1991.
[10] R. Gerson, T.C. Marshall, Dielectric breakdown of porous ceramics, J. Appl. Phys. 30 (1959) 1650–1653.